FULL PAPER

Selective Enhancement of Photoluminescence in Filled Single-Walled Carbon Nanotubes

*Xianjie Liu, Hans Kuzmany, Paola Ayala, Matteo Calvaresi, Francesco Zerbetto, and Thomas Pichler**

The insertion of organometallic molecules into the hollow core of single-walled carbon nanotubes can drastically change their properties. Using biocompatible standardized suspensions of pristine, opened, and filled nanotubes, a very selective enhancement of the photoluminescence and optical absorption is observed. Via ferrocene encapsulation, the PL signal increases almost by a factor of three for tubes with chiralities such as (8,6) and (9,5). This behavior is attributed to a local electron charge transfer from the ferrocene molecules that balances out the p-type doping of the nanotubes resulting from the modified charge distribution of the surfactant molecules and the opening process. The near infrared photoluminescence of the nanotubes in solution is strongly enhanced when ferrocene is encapsulated. The diameter-dependent charge transfer is additionally confirmed by first principles calculations. These findings highlight an essential ingredient to optimize the application of solvated nanotubes, for instance, as in–vivo near infrared sensors in biomedical research.

1. Introduction

The unique one-dimensional nanostructural and electronic properties of single-walled carbon nanotubes (SWCNTs) have stimulated worldwide investigation towards their perspective applications.[1] There is a special interest in the use of semiconducting tubes for the construction of nanoscale devices[2] and applications in fields like biomedicine,[3] where the optical properties associated to the electronic density of states at the van Hove singularities (vHS) of SWCNTs are crucial. They are responsible for a highly selective and sensitive resonant optical absorption (OAS), photoluminescence (PL) and Raman responses.[1,4] Additionally, the excitonic optical band gap of SWCNTs is inversely proportional to their diameter. For nanotubes between 0.8–2 nm the first excitonic transition is in the near infrared (NIR) spectral range, while the second and third are in the visible and UV ranges, respectively. In this context, complementary to OAS, the discovery of a structured PL from isolated semiconducting SWCNTs in solution triggered the study of individual semiconducting nanotubes with defined chirality (n,m).[5] Especially, SWCNTs with an energy gap around 1 eV and a corresponding PL response in the NIR are widely studied. Since blood and tissues are transparent in this spectral range, very promising biomedical applications are envisaged.[3] Therefore, it is not surprising that studies of SWCNTs functionalized with respect to water solubility, biocompatibility and their application in biological imaging and sensing have been remarkably propelled in the last years.[3,6,7]

Although bright NIR emission of SWCNTs has been observed, there is still a debate concerning their emission quantum yields. Reported values range from 0.01% to 7%,[5,8–12] from which, free-standing SWCNTs exhibit the highest values.[8] The PL quantum yield of individual SWCNTs strongly depends on the environment and functionalization, which complicates the production of a biocompatible and water soluble suspension of individual functionalized SWCNTs that retain a bright NIR fluorescence. Not surprisingly, functionalization methods for SWCNTs with respect to water solubility, biocompatibility and their application in biological imaging and sensing have been remarkably propelled in the last years.[3,6,7] The findings reported in the present manuscript highlight an essential ingredient to optimize the application of solvated nanotubes, for instance, as in–vivo near infrared sensors in biomedical research.

Comparing the PL quantum yield of freestanding individual SWCNTs in vacuum, the values for surfactant-stabilized water–soluble SWCNTs remain poor, except where reducing agents are added to solvated tubes to enhance the PL.[12] Covalent sidewall functionalization,[13] as well as functionalization by water filling decrease the PL response of the solvated SWCNTs,[13–15] because it is extremely sensitive not only to charge transfer but also to hybridization. PL quenching occurs either by the presence of metallic SWCNTs, by adsorbed metallic particles, or by covalent and non-covalent functionalization. This structure-dependent luminescence of semiconducting SWCNTs on functionalization and environment has been extensively studied with the goal to monitor any electronic perturbation and the

Dr. X. Liu, Prof. H. Kuzmany, Dr. P. Ayala, Prof. T. Pichler
Faculty of Physics, University of Vienna
Strudlhofgasse 4, 1090 Vienna, Austria
E-mail: thomas.pichler@univie.ac.at
Dr. M. Calvaresi, Prof. F. Zerbetto
University of Bologna
Institute of Inorganic Chemistry
40126 Bologna, Italy

DOI: 10.1002/adfm.201200224

corresponding shifts of the excitonic transition energies.[16–19] Indeed, the controlled functionalization of SWCNTs opens various possibilities to tune the electronic properties and to promote PL visualization. Although controlling the charge transfer to/from semiconducting SWCNTs is a promising way to modify the PL response, most previous studies deal with either covalent attachment of electron donor/acceptor functional groups, or with non–covalent modification.[6,20] An additional disadvantage of such methods is the introduction of non-biocompatible components in solvated SWCNTs and in most of these cases the PL quantum yield is reduced. Only ozone treated SWCNTs in solution exhibit a small increase of the PL response by a sidewall reaction accompanied by a shift in the transition energies, as recently reported.[19] All this happens when we consider the functionalization of the outer side of the SWCNTs, but the hollow space inside the tubes also provides possibilities to modify the tube properties.[21,22] Surprisingly much less has been reported on the PL response of filled nanotubes. The available literature mostly considers big molecules like C_{60} introduced into large diameter SWCNTs, which are not optimum for bio applications.[23] In this regard, selecting molecules with sizes that fit into the inner core of small diameter tubes (ideally between 0.8–1.2 nm) should promote non-covalent interaction preserving the SWCNTs' intrinsic 1D electronic properties. Studies have shown the formation novel hybrid structures by inserting exotic molecules such as organometallic compounds in high yield into small diameter nanotubes, which drastically change their properties.[24] Theoretical work predicted that depending on its electron affinity, the inserted molecule can transfer charge to/from the outer tube, modifying the SWCNTs' electronic properties in a controlled manner even at a molecular level.[25] Nanotube filling can overcome the instability and insolubility of dopants assisted by the effective host nanotube shielding. The great progress related to this method is illustrated by the high yield encapsulation of metallocenes inside SWCNTs with various diameters, such as the work reported in references.[24,26] Note also that if the hollow space inside SWCNTs is seen as the ideal site to perform nanochemical reactions, tracing them makes possible tailoring the charge transfer (p- and n-type) between metallocenes and the tube.[27,28] This provides a unique tunable and reproducible charge transfer interaction between molecules and SWCNTs, without modifications of the 1D vHS response and without influencing their biocompatibility.

This contribution shows for the first time that functionalization with the organometallic compound ferrocene represents an ideal pathway to selectively enhance the PL response in SWCNTs. Using standardized suspensions of pristine, opened and ferrocene filled HiPCo nanotubes, we demonstrate that the optical absorption and the PL response not only strongly depend on the nanotube chirality and diameter, but also on the ferrocene molecules encapsulated in the hollow core. Two-dimensional (2D) PL maps show clearly five different regions of interaction regarding the actual nanotube diameter and chirality. Concomitant to previous results, these regions can be unambiguously assigned to either diameter dependent selective oxidation as well as water filling or to the influence of filling by the organometallic ferrocene molecules. For semiconducting nanotubes with indices (8,6) and (9,5) we find a strong enhancement of the PL response up to a factor of three after filling. These tubes owe a diameter close to the minimal value, which allows them to be filled by ferrocene molecules, i.e. 0.9 nm. The same enhancement for OAS at the first excitonic interband transition indicates that the interaction between the ferrocene molecules and nanotubes yields a local charge transfer, which balances out the charge distribution of the surfactant molecules. This charge transfer was analyzed by ab-initio simulations using a Mulliken population analysis of density functional theory (DFT) calculations and confirmed that it is most efficient when the diameter of the nanotubes is close to the size of the ferrocene molecule and two times the van der Waals radius.

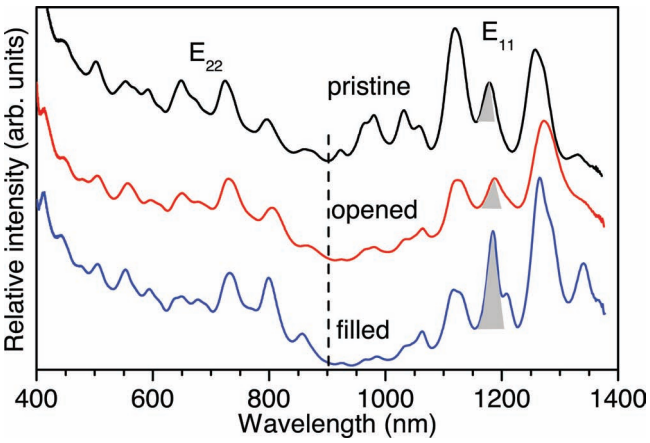

Figure 1. Optical absorption for pristine (black), opened (red), and filled (blue) nanotubes, as suspended in bile salt water solution. All spectra were normalized[13,29] at the position of the minimum between E_{11} and E_{22}, as indicated by the dashed line. The grey area highlights the E_{11} peak, which shows the strongest enhancement with filling.

2. Results and Discussion

The suspensions used in our experiments were pristine, opened and ferrocene filled HiPCo nanotubes. The processes to open, fill and determine the filling ratio are fully described in the supplementary information provided. We start here with a comparison of the OAS of suspended individual tubes. The spectra obtained from pristine, opened and filled SWCNTs are shown in **Figure 1** from top to bottom and they were normalized at the position of the minimum between E_{11} and E_{22}, as indicated by the dashed line.[13,29] According to the absorption energy, the peaks E_{11} and E_{22} can be assigned to the first and second excitonic transitions between vHs of semiconducting SWCNTs, respectively. The changes of spectral features of the first interband transition in the opened tubes due to oxidation and doping effects also appear. If we look at the optical absorption peaks at wavelengths between 900 and 1100 nm, they were obviously suppressed for the opened and filled tubes in comparison to the pristine ones. On the other hand, the intensity of the corresponding E_{22} is unchanged. This significant lowering in the aforementioned range can be attributed to the reduced abundance of tubes with that corresponding signal after opening. Note that it has been suggested that the red-shift of the E_{11} transitions in the opened tubes can be due to water

filling, because it induces a strong change of dielectric background.[30] This is a solid proof, which distinctly illustrates that smaller tubes with higher curvature are more reactive than tubes with larger diameter. The end caps of SWCNTs must be opened before ferrocene filling and we cannot forget that the oxidation in air is used to remove the caps because they are more reactive compared to the nanotube sidewalls due to their higher curvature.[31] However, for the same reason tubes with ultra small diameter are also sensitive to the oxidation process.[32] The influence of the opening process and the subsequent water filling on the PL response still need to be clarified although it has been reported to some extent that they strongly influence the optical and PL response.[30] The SWCNTs' opening induces p-type doping attributed to adsorbed oxygen at ambient conditions and carbon-oxygen bonds formed during thermal treatments.[33] Such doping depletes the electrons in the valence band of SWCNTs and induces a downshift of the Fermi level. Correspondingly, some optical allowed excitonic interband transitions between the valence and conduction band of SWCNTs are suppressed. This doping effect can be very localized and independent from the diameters. It is also different from pure charge transfer p-type doping where only charge from the highest valence band is taken, and therefore it influences the spectral features of the E_{11} region for all types of SWCNTs simultaneously. This also explains the change of optical intensity for peaks between 1100 and 1250 nm. Furthermore, there is no obvious shift of the optical absorption peak and in the corresponding fluorescence response. The doping by opening is also different from doping by strong ozone based oxidation, where nanotube solutions are first exposed to ozone and subsequently to light. In this way oxygen is absorbed on the wall of a nanotube and traps mobile excitons.[19] In contrast to the results depicted in Figure 1 this strong oxygen doping modifies the NIR band gaps in fluorescent SWCNTs. Analyzing the ferrocene filling, the red shift of E_{11} is retained and absorption of selected SWCNTs is strongly enhanced. This is highlighted in Figure 1 by the grey area with the peak at 1180 nm. Also some of the peaks that overlap those additionally enhanced peaks can be tentatively assigned to the (8,6), (8,7), (9,5), (10,5), and (11,1) tubes. This is a first indication of compensation due to p-type doping via the charge transfer from the encapsulated ferrocene molecules to the nanotubes.

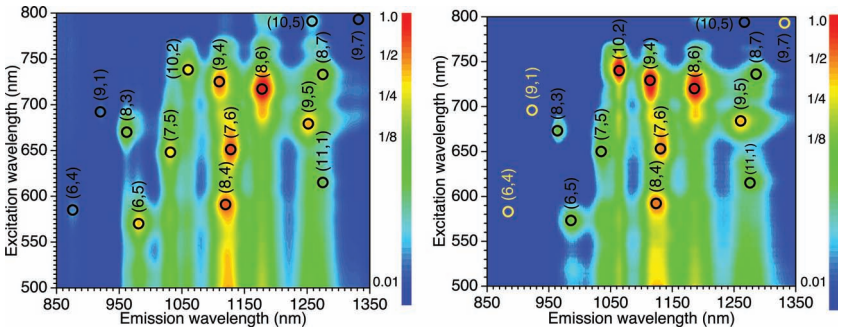

Figure 2. Maps for pristine tubes (left) and opened SWCNTs (right), respectively. All tubes were suspended in bile salt aqueous solution. The PL intensity is plotted on a logarithmic scale after normalizing to the optical density at 900 nm. The yellow circles show PL peaks of SWCNTs, which disappeared in the opened sample but are present in the pristine material.

The results of the 2D PL maps of the pristine and opened tubes are depicted in **Figure 2**, again after the normalization to the optical density at 900 nm. In the corresponding contour plots, the color code describes the intensity of the peaks associated with the emission from the E_{11} transition after excitation in the second interband transition E_{22}. The assignment of the specific chiralities for each peak was performed following the empirical relations from Bachilo et al.[34] It is obvious that significant changes of spectral features in the PL maps happen for smaller diameter SWCNTs. For example, tubes (8,3), (6,5), and (7,5) exhibit a reduced PL intensity after opening, whereas the emission feature of nanotubes (6,4) and (9,1) completely disappeared. This vanishing can be again associated with the fact that smaller tubes are more reactive with oxygen in the opening process.[32] The comparison reveals on the other hand an increase of PL signals from larger diameter tubes after opening. The relative PL intensity of special chirality SWCNTs is also altered after opening, since the oxidation process eliminates some SWCNTs leading to a revision of their diameter distribution as the relative abundance of each tube is changed. For instance tubes (10,2) and (9,4) are more abundant in the opened material than in the pristine material. In the opened tubes, the resonance for excitation and the fluorescence peak positions were slightly, but non-uniformly, red-shifted compared to their position in the pristine SWCNTs. The former red shifts by about 3 nm, while the latter is downshifted by 6 nm on average. Such red-shifts can be explained by the presence of liquids inside the opened SWCNTs.[16] The tube-filling with surfactants can be ruled out due to the small tube diameter of only about 1 nm.[35] The encapsulated water causes a reduction of electron-electron repulsion and exciton binding energy by dielectric screening effects, which results in the observed red shifts.[30] The red-shift of the emission wavelength shows a dependence on the nanotube diameter. Larger diameter nanotubes exhibit a stronger downshift, since they are more favorable for filling than smaller tubes.[36] Considering the size of the ferrocene molecule and van der Waals distance, the smallest diameter of a nanotube which can be filled by ferrocene is around 0.9 nm, as proved by multifrequency Raman results and molecular dynamics calculations.[26] Therefore, only few tubes in the PL response of Figure 2, namely the tubes with chirality (8,6), (9,5), (8,7), (11,1), and (10,5) are large enough for ferrocene encapsulation. Smaller diameter semiconducting tubes are not able to host ferrocene molecules. This is confirmed in the 2D PL contour map of ferrocene filled nanotubes as shown in **Figure 3**. The distinct feature is the strong enhancement of the emission for longer wavelengths, especially emission features from tubes (8,6) and (9,5), while the emission from tubes (10,2) and (9,4) is dramatically decreased. The fluorescence peak position of ferrocene filled SWCNTs are clearly red-shifted like the emission peaks of opened water filled tubes. The luminescence is very close (nearly the same peak shift) in smaller tubes without ferrocene filling and opened tubes, which is not surprising since both were only filled by water. On the other hand, the

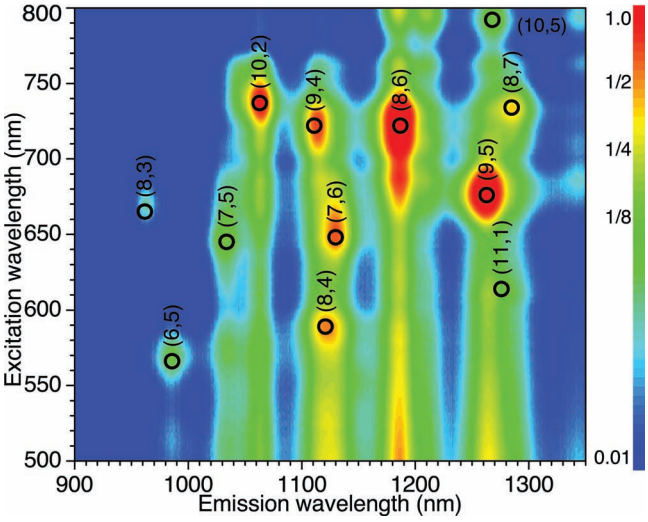

Figure 3. 2D PL excitation–emission contour plot for ferrocene filled SWCNTs dispersed in bile salt water solution. The PL intensity is plotted in a logarithmic scale after normalizing to the optical density at 900 nm.

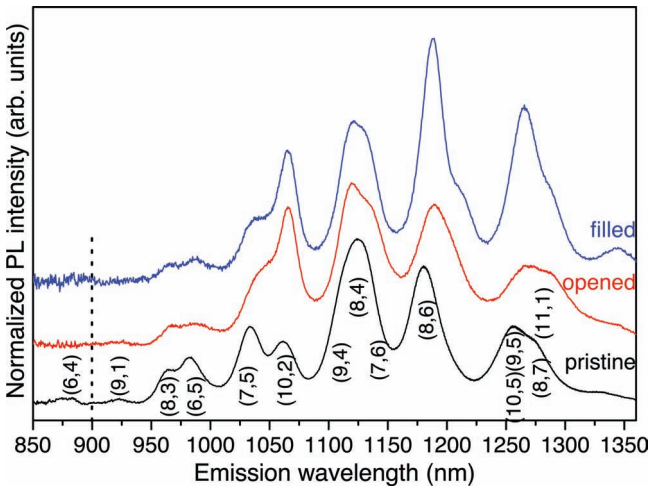

Figure 4. Spectra integrated for excitations between 500 and 800 nm for pristine (black), opened (red), and ferrocene filled SWCNTs (blue), respectively. The dashed line indicates the normalization point. The chirality assignment for the emission spectra is shown.

emission peak from ferrocene filled tubes is 2 nm redshifted compared to water filled tubes. The excitation from ferrocene filled tube shows a blueshift by about 2 nm, which further confirms the different effect of encapsulated ferrocene and water on PL. Regarding the relative PL quantum yield, we consider the observed signals in the PL maps, which represent the abundance of the corresponding nanotube species as well as their intrinsic PL intensities. The peak height or the integrated intensity of the signal can be used to discuss the PL response.[9] However, to find the structure-dependent intrinsic PL quantum yield, excitonic transitions must also be taken into account to extract abundances of the different semiconducting nanotube species.[37] Here, for simplicity, only the relative variation of PL amplitude is considered. In our case all emission spectra are summed up for excitation wavelengths between 500 10 and 800 nm in order to extract the average relative PL cross-section. Analogous to the optical absorption, the summed spectra of the pristine, opened and filled nanotubes are again normalized at 900 nm in order to account for the different optical density. This is the most accurate normalization since there are no emission peaks and therefore, only contribution from the static dielectric background is present. This was also used to normalize the PL intensity in the color code of the 2D PL maps in Figure 2 and 3. **Figure 4** depicts the integrated PL response (integrating the excitation energy between 500 and 800 nm) normalized again to the optical density at 900 nm. There is a remarkable enhancement of the intensity for filled SWCNTs at emission wavelengths around 1190 nm and 1270 nm. The strongest enhancement is found for the tubes with chirality (8,6) and (9,5). This integrated PL response complements the OAS results described before.

To elucidate the changes in the PL intensity in more detail, in **Figure 5**a we have also plotted the relative PL intensity ratios between the pristine, opened and filled nanotubes as a function

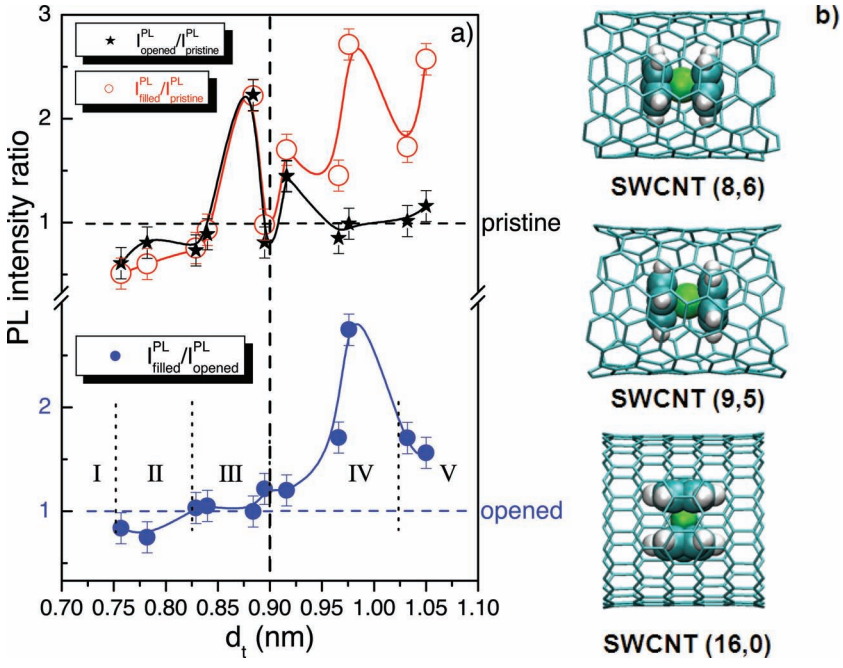

Figure 5. a) Top: PL intensity of opened (★) and filled (○) tubes in relation to pristine nanotubes as a function of the tube diameter. Bottom: Ratio between the filled (●) and opened tubes as a function of tube diameter. The dashed line indicates the smallest diameter for which tubes can be filled with ferrocene. Different regions are separated by vertical dotted line marked as I, II, III, IV, and V. b) Optimized geometries for ferrocene filled into SWCNTs with molecules aligned lying (chirality (8,6) and (9,5)) and molecules aligned standing (chirality (16,0)).

of the tube diameter $\left(\frac{I^{PL}_{opened}}{I^{PL}_{pristine}}, \frac{I^{PL}_{filled}}{I^{PL}_{pristine}}, \text{and } \frac{I^{PL}_{filled}}{I^{PL}_{opened}}\right)$. The Roman numbers identify five different diameter regions. Regarding the PL intensity ratio between opened and pristine tubes, the ones smaller than 0.75 nm were etched away during the opening process, and therefore have zero PL yield. This is highlighted in zone I. For tube diameters smaller than 0.82 nm, opened tubes have lower PL intensity than pristine ones, assigned to the non-radiative recombination from the defects in the opened tubes generated in oxidation process (zone II). Opened and pristine specie with diameters larger than 0.82 nm have almost the same PL intensity, except for two kinds with 0.88 and 0.91 nm, assigned to (10,2) and (9,4), respectively. The PL intensity enhancement in these cases accounts the dramatic increase of relative abundance resulting from the opening process (zone III). Here the tubes are still too small to allow ferrocene encapsulation, but they can be filled with water. With increasing tube diameters, the ferrocene molecules go inside the tubes and the PL intensity is dramatically enhanced. This is shown in zones IV and V, where zone IV is the optimum region. The change of PL intensity ratio between the filled tubes and the pristine and opened tubes clearly indicates a threshold at 0.90 nm (there is no PL enhancement below 0.90 nm but it is strong for tubes larger than 0.90 nm). Additionally, the minimum diameter of tubes to host ferrocene is found to be 0.90 nm. The PL enhancement induced by ferrocene filling is clearly demonstrated in the lower panel of Figure 5a and it can be as high as a factor of three. Since the filled and the opened materials have the same relative nanotube abundance, we can focus only on ratio between filled and opened tubes as a function of tube diameter (zones IV and V). In the PL map in Figure 3, the signal increases to about 170% and 270% for tubes (8,6) and (9,5), compared to opened tubes' PL intensity. For the (8,7) and (10,5) tubes there is still increase to 160% and 175% after filling as compared to the pristine SWCNTs' intensity. This enhancement is also clearly depicted in the optical absorption response of the E_{11} transition, as shown in Figure 1.

Strong absorption peaks in the spectrum corresponding to the ferrocene filled tubes were found at 1180 nm and 1270 nm (grey shaded area) with a blue shift compared to the response for the opened tubes. This charge transfer between ferrocene and nanotubes of different diameters has been reported experimentally and theoretically.[27,38,39] For instance, a –0.0067 e-/Å electron charge transfer was shown in a 1.4 nm tube.[27] Molecular dynamics calculations demonstrate that the optimal diameter at which ferrocene filling starts is about 0.9 nm (0.05 nm smaller than that observed in Raman, where only tubes in which ferrocene can be converted into inner tubes can be detected).[26] Details about these mentioned Raman measurements can be found in the supplementary information. In our experiments, the smallest detected inner tube had (4,3) chirality. Here, notice that the carbon atoms from the decomposed ferrocene molecules would not be able to form a stable inner tube if the diameter would be too small to allow the closing of an inner tube. Monitoring the PL intensity immediately after filling, we could confirm the filling of tubes which are too small to host a stable inner tube, which cannot be detected by Raman spectroscopy. We corroborated that the observed limiting tube diameter of 0.9 nm for ferrocene filling is in perfect agreement with the theoretical predictions.[26] When the diameter is increased beyond 0.9 nm, the molecules can enter and form a linear chain with orientation parallel to the tube axis. At about 0.97 nm a maximum increase of the PL intensity is obtained. With diameters above 1 nm, the ferrocene orientation is such that the axes of the molecules are perpendicular to the tube axis. Both facts are expected to significantly modify the charge transfer from the ferrocene to the nanotubes. The PL intensity is influenced by the change of orientation as indicated in zone V. To evaluate the charge transfer from ferrocene to the nanotube in different orientations, we performed a Mulliken-population analysis. Considering the experimental results, (8,6), (9,5) and (16,0) tubes were used to exemplify this. Their diameters are appropriate for filling in the parallel and perpendicular geometry, respectively. The configurations are shown in Figure 5b and represent typical tubes of the zone IV and V. For both orientations we observe a transfer of electrons from ferrocene to the nanotube. For the (8,6) and (9,5) tubes the charge transfer is –0.0119 and –0,0124 e-/Å correspondingly, while for the (16,0) the value is –0.0106 e-/Å. In all cases this charge transfer is more than twice as high as observed explicitly by photoemission experiments using 1.4 nm tubes.[27] From this analysis we can assert that the selective increase of the PL intensity is related to the charge transfer from ferrocene to the nanotubes. The n-type doping from ferrocene compensates p-type doping from the opening process and the surfactant molecules. This also explains the different enhancement factors for different chiralities. The highest electron charge transfer (e-/Å) is observed when the molecules are optimally oriented, which also gives the strongest enhancement of the PL. The response of filled individual tubes in solution is still slightly lower compared to the results in freestanding SWCNT,[8] which indicates that the maximum charge transfer from ferrocene defines the lower boundary to balance out the p-type doping resulting from opening and solvatation. It is then inferable that using different fillers with optimized diameters can provide an even stronger charge transfer, enabling tailoring the PL response in solution to the limit given by the freestanding SWCNT. It is interesting to compare the response from ferrocene filling with C_{60} filled SWCNTs, where no charge transfer occurs.[40,41] From the weak van der Waals interaction between C_{60} and nanotubes, changes are observed in the vibrational and optical response like a shift in the pentagonal pinch mode in C_{60}[40] and a strong spectral shift of the excitation and emission energies in the PL maps by up to 100 meV (with no obvious change in PL intensity), attributed to local strain effects and hybridization of the SWCNTs and the C_{60}.[23] This differs clearly from ferrocene filled SWCNTs, where there is strong charge transfer, but the corresponding fluorescent spectral shift is less than 10 meV, indicating that ferrocene filling does not lead to strong distortion of the outer tubes, which would yield a strong modification of the gap. The PL spectral intensity enhancement is rather assigned to the formation of a novel hybrid complex balancing the p-type doping from the opening and solvatation processes.

3. Conclusions

Summarizing, we demonstrate a clear pathway to enhance the near infrared PL of SWCNTs in solution by inserting

organometallic molecules, particularly useful for biological imaging, where bright SWCNT–fluorescence with high biocompatiblity is required. The ferrocene encapsulation increases the PL signal almost by a factor of three in SWCNTs with diameters close to 0.9 nm, indicating that the interaction between ferrocene and those nanotubes yields a local diameter dependent charge transfer, which balances out the p-type doping from the opening and the charge distribution of the surfactant molecules. First principles calculations suggest an orientation of the molecules inside the tubes. These filling reactions are applicable to other non-biocompatible donor and acceptor molecules with equivalent diameters allowing tailoring the photoluminescence, which is a crucial ingredient to optimize the application of solvated SWCNTs as in–vivo near infrared sensors in biomedical research.

4. Experimental Section

Because of their broad diameter distribution and a mean diameter of around 1 nm, commercially available HiPCo (high pressure decomposition CO) SWCNTs were used in this study. Purification by vacuum annealing and centrifugation were applied to obtain what was used as the pristine starting material. In a second step, the tubes were opened by heating a buckypaper in air up to 420 °C for 20 min. As a third step, filling with ferrocene was achieved by heating a mixture of ferrocene and opened nanotubes inside a vacuum ($<5 \times 10^{-6}$ mbar) sealed quartz tube at 400 °C for 72 h.[24,26] The non-encapsulated ferrocene was removed by dynamic vacuum annealing at 400 °C for 1 h.[26] Additionally, after the PL experiments, the ferrocene filled SWCNTs were converted into double-walled carbon nanotubes to verify the filling ratio. Details about this procedure and the filling ratios are given in the supplementary information. To obtain well-isolated individual nanotubes, the samples were dispersed in deionized water with the help of 2% w/v bile salts (Sigma Aldrich) under ultrasonication (Branson Sonifier 450) and subsequent centrifugation (Thermal Scientific 1 000 000 g).[42] Their supernatant (50%) rich with isolated nanotubes was collected as target material for this study. OAS data were collected using a Bruker VERTEX 80v Fourier transform spectrometer. PL measurements were carried out with a Nanolog (Horiba Jobin Yvon) spectrometer with emission wavelengths from 800 to 1360 nm. All measurements were done at room temperature. Normalization of the different suspensions with respect to their optical density was achieved by taking the background between the first and second optical transition as reference.[13,29] Furthermore, in order to evaluate the charge transferred from ferrocene to the nanotube for various molecular orientations, Mulliken-population analysis of DFT calculations at the PBE/6- 31G⋆ level were performed. The DFT calculations were carried out with the Gaussian[43] series of programs using the PBE functional.[44] PBE has already proved to be efficient both in describing transition-metal-doping in single-walled carbon nanotubes[45] and in determining the ground state geometric and electronic structure of ferrocene.[46] The 6-31G⋆ basis set was used.[47]

The Mulliken analysis allows quantifying the charge transfer between the ferrocene molecule and the nanotube.[48] A cluster model approach was selected for the description of the nanotubes. Compared with other first-principles approaches, the cluster model has advantages in computational speed and physical transparency and provides a description of local bonding information, charge transfer, and related properties. Electronic structure calculations frequently invoke periodic boundary conditions to obtain electrostatic potentials. For systems that are electronically charged, or which contain dipole (or higher) moments, this artifice introduces spurious potentials due to the interactions between the system and multipole moments of its periodic images in aperiodic directions. Charged systems are particularly problematic since their electrostatic energy would be divergent. The geometries were taken from minimized structures obtained by Quenched Molecular Dynamics.[26]

Supporting Information

Supporting Information is available from the Wiley Online Library or from the author.

Acknowledgements

Financial support by the FWF project P21333-N20 is acknowledged. P.A. was supported by a Marie Curie Intra European Fellowship within the 7th European Community Framework Programme.

Received: January 24, 2012
Published online: April 23, 2012

[1] *Advanced Topics in the Synthesis, Structure, Properties and Applications*, (Eds: A. Jorio, G. Dresselhaus, M. S. Dresselhaus) Springer-Verlag, Berlin, Germany **2008**.
[2] J. A. Misewich, R. Martel, P. Avouris, J. C. Tsang, S. Heinze, J. Tersoff, *Science* **2003**, *300*, 783.
[3] Z. Liu, S. Tabakman, K. Welsher, H. J. Dai, *Nano Res.* **2009**, *2*, 85.
[4] H. Kataura, Y. Kumazawa, Y. Maniwa, I. Umezu, S. Suzuki, Y. Ohtsuka, *Synth. Met.* **1999**, *103*, 2555.
[5] M. J. O'Connell, S. M. Bachilo, C. B. Huffman, V. C. Moore, M. S. Strano, E. H. Haroz, K. L. Rialon, P. J. Boul, W. H. Noon, C. Kittrell, J. P. Ma, R. H. Hauge, R. B. Weisman, R. E. Smalley, *Science* **2002**, *297*, 593.
[6] P. W. Barone, S. Baik, D. A. Heller, M. S. Strano, *Nat. Mater.* **2005**, *4*, 86.
[7] K. Welsher, Z. Liu, S. P. Sherlock, J. T. Robinson, Z. Chen, D. Daranciang, H. Dai, *J. Nat. Nanotechnol.* **2009**, *4*, 773.
[8] J. Lefebvre, D. G. Austing, J. Bond, P. Finnie, *Nano Lett.* **2006**, *6*, 1603.
[9] M. Jones, C. Engtrakul, W. K. Metzger, R. J. Ellingson, A. J. Nozik, M. J. Heben, G. Rumbles, *Phys. Rev. B* **2005**, *71*, 115426.
[10] D. A. Tsyboulski, J. D. R. Rocha, S. M. Bachilo, L. Cognet, R. B. Weisman, *Nano Lett.* **2007**, *7*, 3080.
[11] J. Crochet, M. Clemens, T. Hertel, *J. Am. Chem. Soc.* **2007**, *129*, 8058.
[12] A. J. Lee, X. Y. Wang, L. J. Carlson, J. A. Smyder, B. Loesch, X. M. Tu, M. Zheng, T. D. Krauss, *Nano Lett.* **2011**, *11*, 1636.
[13] C. Backes, U. Mundloch, A. Ebel, F. Hauke, A. Hirsch, *Chem. Eur. J.* **2010**, *16*, 3314.
[14] V. C. Moore, M. S. Strano, E. H. Haroz, R. H. Hauge, R. E. Smalley, J. Schmidt, Y. Talmon, *Nano Lett.* **2003**, *3*, 1379.
[15] S. Cambre, W. Wenseleers, *Angew. Chem. Int. Ed.* **2011**, *50*, 2764.
[16] J. Lefebvre, J. M. Fraser, Y. Homma, P. Finnie, *Appl. Phys. A* **2004**, *78*, 1107.
[17] P. Finnie, Y. Homma, J. Lefebvre, *J. Phys. Rev. Lett.* **2005**, *94*, 247401.
[18] A. V. Naumov, S. M. Bachilo, D. A. Tsyboulski, R. B. Weisman, *Nano Lett.* **2008**, *8*, 1527.
[19] S. Ghosh, S. M. Bachilo, R. A. Simonette, K. M. Beckingham, R. B. Weisman, *Science* **2010**, *330*, 1656.
[20] U. Hahn, S. Engmann, C. Oelsner, C. Ehli, D. M. Guldi, T. Torres, *J. Am. Chem. Soc.* **2010**, *132*, 6392.
[21] B. W. Smith, M. Monthioux, D. E. Luzzi, *Nature* **1998**, *396*, 323.

[22] T. Takenobu, T. Takano, M. Shiraishi, Y. Murakami, M. Ata, H. Kataura, Y. Achiba, Y. Iwasa, *Nat. Mater.* **2003**, *2*, 683.
[23] T. Okazaki, S. Okubo, T. Nakanishi, S. K. Joung, T. Saito, M. Otani, S. Okada, S. Bandow, S. Lijima, *J. Am. Chem. Soc.* **2008**, *130*, 4122.
[24] H. Shiozawa, T. Pichler, A. Gruneis, R. Pfeiffer, H. Kuzmany, Z. Liu, K. Suenaga, H. Kataura, *Adv. Mater.* **2008**, *20*, 1443.
[25] J. Lu, S. Nagase, D. P. Yu, H. Q. Ye, R. S. Han, Z. X. Gao, S. Zhang, L. M. Peng, *Phys. Rev. Lett.* **2004**, *93*, 116804.
[26] W. Plank, R. Pfeiffer, C. Schaman, H. Kuzmany, M. Calvaresi, F. Zerbetto, J. Meyer, *ACS Nano* **2010**, *4*, 4515.
[27] H. Shiozawa, T. Pichler, C. Kramberger, A. Grüneis, M. Knupfer, B. Büchner, V. Zolyomi, J. Koltai, J. Kürti, D. Batchelor, H. Kataura, *Phys. Rev. B* **2008**, *77*, 153402.
[28] H. Shiozawa, T. Pichler, C. Kramberger, M. Rümmeli, D. Batchelor, Z. Liu, K. Suenaga, H. Kataura, S. R. Silva, *Phys. Rev. Lett.* **2009**, *102*, 046804.
[29] J. A. Fagan, J. R. Simpson, B. J. Bauer, S. H. D. Lacerda, M. L. Becker, J. Chun, K. B. Migler, A. R. H. Walker, E. K. Hobbie, *J. Am. Chem. Soc.* **2007**, *129*, 10607.
[30] T. Ando, *J. Phys. Soc. Jpn.***2004**, *73*, 3351.
[31] H. Kataura, Y. Maniwa, T. Kodama, K. Kikuchi, K. Hirahara, K. Suenaga, S. Iijima, S. Suzuki, Y. Achiba, W. Kratschmer, *Synth. Met.* **2001**, *121*, 1195.
[32] Y. Miyata, T. Kawai, Y. Miyamoto, K. Yanagi, Y. Maniwa, H. Kataura, *Phys. Status Solidi B* **2007**, *244*, 4035.
[33] K. Bradley, S. H. Jhi, P. G. Collins, J. Hone, M. L. Cohen, S. G. Louie, *Phys. Rev. Lett.* **2000**, *85*, 4361.
[34] S. M. Bachilo, M. S. Strano, C. Kittrell, R. H. Hauge, R. E. Smalley, R. B. Weisman, *Science* **2002**, *298*, 2361.
[35] E. J. F. Carvalho, M. C. dos Santos, *ACS Nano* **2010**, *4*, 765.
[36] W. Wenseleers, S. Cambre, J. Culin, A. Bouwen, E. Goovaerts, *Adv. Mater.* **2007**, *19*, 2274.
[37] S. Heeg, E. Malic, C. Casiraghi, S. Reich, *Phys. Status Solidi B* **2009**, *246*, 2740.
[38] V. M. Garcia-Suarez, J. Ferrer, C. J. Lambert, *Phys. Rev. Lett.* **2006**, *96*, 106804.
[39] E. L. Sceats, J. C. Green, *J. Chem. Phys.* **2006**, *125*, 154704.
[40] T. Pichler, H. Kuzmany, H. Kataura, Y. Achiba, *Phys. Rev. Lett.* **2001**, *87*, 267401.
[41] H. Rauf, H. Shiozawa, T. Pichler, M. Knupfer, B. Buchner, H. Kataura, *Phys. Rev. B* **2005**, *72*, 245411.
[42] W. Wenseleers, I. I. Vlasov, E. Goovaerts, E. D. Obraztsova, A. S. Lobach, A. Bouwen, *Adv. Funct. Mater.* **2004**, *14*, 1105.
[43] M. J. Frisch, G. W. Trucks, H. B. Schlegel, G. E. Scuseria, M. A. Robb, J. R. Cheeseman, G. Scalmani, V. Barone, B. Mennucci, G. A. Petersson, H. Nakatsuji, M. Caricato, X. Li, H. P. Hratchian, A. F. Izmaylov, J. Bloino, G. Zheng, J. L. Sonnenberg, M. Hada, M. Ehara, K. Toyota, R. Fukuda, J. Hasegawa, M. Ishida, T. Nakajima, Y. Honda, O. Kitao, H. Nakai, T. Vreven, J. A. Montgomery Jr., J. E. Peralta, F. Ogliaro, M. Bearpark, J. J. Heyd, E. Brothers, K. N. Kudin, V. N. Staroverov, R. Kobayashi, J. Normand, K. Raghavachari, A. Rendell, J. C. Burant, S. S. Iyengar, J. Tomasi, M. Cossi, N. Rega, J. M. Millam, M. Klene, J. E. Knox, J. B. Cross, V. Bakken, C. Adamo, J. Jaramillo, R. Gomperts, R. E. Stratmann, O. Yazyev, A. J. Austin, R. Cammi, C. Pomelli, J. W. Ochterski, R. L. Martin, K. Morokuma, V. G. Zakrzewski, G. A. Voth, P. Salvador, J. J. Dannenberg, S. Dapprich, A. D. Daniels, Ö. Farkas, J. B. Foresman, J. V. Ortiz, J. Cioslowski, D. J. Fox, Gaussian 09, Gaussian, Inc., Wallingford, CT **2009**.
[44] J. P. Perdew, K. Burke, M. Ernzerhof, *Phys. Rev. Lett.* **1996**, *77*, 3865.
[45] Y. K. Chen, L. V. Liu, W. Q. Tian, Y. A. Wang, *J. Phys. Chem. C* **2011**, *115*, 9306.
[46] S. Scuppa, L. Orian, D. Dini, S. Santi, M. Meneghetti, *J. Phys. Chem. A* **2009**, *113*, 9286.
[47] V. A. Rassolov, J. A. Pople, M. A. Ratner, T. L. Windus, *J. Chem. Phys.* **1998**, *109*, 1223.
[48] R. S. Mulliken, *J. Chem. Phys.* **1955**, *23*, 1833.